

Thermally driven hopping and electron transport in amorphous materials from density functional calculations

Tesfaye A Abtew and D A Drabold

Department of Physics and Astronomy, Ohio University, Athens, OH 45701-2979, USA

E-mail: abtew@helios.phy.ohiou.edu and drabold@ohio.edu

Received 17 August 2004

Published 22 October 2004

Online at stacks.iop.org/JPhysCM/16/S5289

doi:10.1088/0953-8984/16/44/025

Abstract

In this paper we study electron dynamics and transport in models of amorphous silicon and amorphous silicon hydride. By integrating the time-dependent Kohn–Sham equation, we compute the time evolution of electron states near the gap, and study the spatial and spectral diffusion of these states due to lattice motion. We perform these calculations with a view to developing *ab initio* hopping transport methods. The techniques are implemented with the *ab initio* local basis code SIESTA, and may be applicable to molecular, biomolecular and other condensed matter systems.

(Some figures in this article are in colour only in the electronic version)

1. Introduction

Mike Thorpe has worked intensely on practically every aspect of the physics of disordered systems, always with an eye toward *general* insights. To many attending this meeting, his work on floppy modes and the entire view of disordered systems it has engendered is the best known single contribution. Yet Mike has also contributed deeply to issues of structure and of theory of spin systems, and with Denis Weaire has offered another cornerstone of understanding of amorphous insulators: the Weaire–Thorpe theorem, which explains the existence of an optical gap in terms of the connectivity of an amorphous covalently bonded network. With characteristic elegance, the problem is formulated in a one-band tight-binding (essentially bond-orbital) picture, and the analysis concludes with an appeal to a theorem of linear algebra. It is a delight in re-reading these papers to see Mike’s lifelong friend, scientific foil and colleague Jim Phillips referenced and his ideas discussed in the context of the work of Thorpe and Weaire [1]. This result has become such a basic part of our thinking that it is worth reading the comments of Ziman [2] on the non-trivial nature of the work.

In this paper, we shall be concerned with mixing two of Michael's favourite things: electron states and vibrational dynamics. The essential underlying physical processes were deduced by Sir Nevill Mott [3], Miller and Abrahams [4] and Conwell [5] in the 1950s; the methods have been nicely updated by Shklovskii and Efros [6]. In this paper we take these ideas seriously, and use current density functional descriptions of electron states, and computational schemes for integrating the time-dependent Schrödinger (Kohn–Sham) equation to work out the consequences of a dynamic lattice on electron states (thermally driven hopping). Phonon-induced delocalization is clearly seen. An accessible explanation of the idea, and a review of the field up to the early 1980s, is given by Zallen [7].

Because of nanoscience and microelectronics, there is currently a renaissance of interest in transport calculations, and creation of predictive theories of transport. While the present theory lacks the rigour of the best current techniques, it is easy to implement and easy to understand. Our scheme also has the strength that it is based upon a *dynamic lattice*, unlike the most sophisticated methods (where one obtains conductivities due to external fields with a frozen lattice). We expect that this additional realism will give improved results for localized states with their large electron–phonon coupling [8], and this gives us cause to hope that the method will have broad utility [9].

2. Methodology

2.1. Electronic structure

In our calculations we used the code SIESTA [10–12] within the local density approximation and the parametrization of Perdew and Zunger [13] for the exchange–correlation functional. To remove core electrons from the calculations, norm conserving Troullier–Martins [14] pseudopotentials factorized in the Kleinman–Bylander [15] form were used. We employed single- ζ (SZ) basis sets [16] where one s orbital for the H valence electron and one s and three p orbitals for the Si valence electrons were used. The Γ point was used to sample the Brillouin zone. To track the time evolution of a given state an additional subroutine has been added to the SIESTA code. In the simulation, 1000 molecular dynamics steps for a time step of 0.50 fs were performed. (We have checked a time step of 0.05 fs and the result does not change.) For this first trial of the approach, we have used a non-self-consistent version of SIESTA, an investigation we shall explore in subsequent work.

Elsewhere [8], it has been shown that the electron–phonon coupling is always large for localized states, which suggests the need for a non-perturbative solution for the time evolution of localized electrons in a dynamic network. In particular, it was shown there that Kohn–Sham eigenvalues conjugate to localized eigenstates may thermally fluctuate by tenths of an electronvolt, *larger than kT* . The spectral and spatial electronic diffusion can be obtained by tracking the time evolution of the state by solving the time-dependent Kohn–Sham equation:

$$i\hbar \frac{\partial}{\partial t} \psi(t) = \hat{H}(t) \psi(t) \quad (1)$$

where \hat{H} is the Hamiltonian operator and $\psi = \sum_i C_i \phi_i$ is the single-electron wavefunction written in the basis of non-orthogonal orbitals $\{\phi_i\}$. The Löwdin transformation is used to convert to an orthonormal basis $\{\varphi_i\}$ which is defined by $\varphi_i = \sum_j (S^{-1/2})_{ij} \phi_j$ where $S_{ij} = \int \phi_i \phi_j d^3r$ is the overlap matrix [17]. With these transformations (1) becomes in an explicit matrix representation

$$i\hbar \frac{\partial}{\partial t} C' = H' C' \quad (2)$$

where $H' = S^{-1/2} H S^{-1/2}$ and $C' = S^{1/2} C$. The time development can be obtained by using the Crank–Nicholson scheme with the approximate evolution operator linking time t to $t + \tau$, where τ is a small time interval between two consecutive time steps:

$$C'(t + \tau) = (1 + i\tau H'(t)/2\hbar)^{-1} (1 - i\tau H'(t)/2\hbar) C'(t). \quad (3)$$

This evolution operator is unitary for any τ (of course it only tracks the correct solution for τ small enough).

The participation ratio, \mathcal{P} , is a quantity that tells us how many sites participate in a given eigenstate. For an ideally localized state $\mathcal{P} = 1$, and for extended states \mathcal{P} could reach the number of atoms N . The inverse of \mathcal{P} is defined as the inverse participation ratio \mathcal{I} . Given the eigenvector $C'_j(R_i)$ for state j which is defined at each site R_i , \mathcal{I} is defined as

$$\mathcal{I}_j = (1/\mathcal{P})_j = \frac{\sum_i |C'_j(R_i)|^4}{(\sum_i |C'_j(R_i)|^2)^2}. \quad (4)$$

Since we are able to get the time evolution of the eigenvector $C'(t)$ from equation (3), the spatial and spectral diffusion of the localized states can be obtained from equation (4). For \mathcal{I} large we have a well localized state; \mathcal{I} small means that the state is extended.

2.2. Structural models

Perhaps both the strength and weakness of our calculation is that we employ fairly realistic structural models of a-Si [18] and a-Si:H [19] (we name these asi-64 and asi:H-138 respectively). The virtue of the approach is that the true topological disorder is encoded into the coordinates of the supercells we employ. Furthermore, the lattice motion is determined from conventional *ab initio* thermal simulation, and thus should also be fairly realistic. The a-Si:H model has no defects; the a-Si model has one pair of coordination (under-coordinated dangling bond and over-coordinated ‘floating’ bond) defects.

The shortcomings are not to be minimized, and arise from the small model sizes, and for low temperatures classical lattice dynamics, rather than a phonon picture, which strictly is needed for $T < \Theta_D$. Our supposition is that the small model size is the most serious deficiency, as only an extremely sparse sampling of the gap and tail states is possible for small models as we discuss here. This limitation appears to be somewhat ameliorated by the large thermally driven fluctuations of the localized states that we do have, but this point needs to be carefully studied in future work.

2.3. Transport theory

At low temperature where the density of states at the Fermi level is finite but states near the Fermi energy are localized, Mott and Davis [20] described the phenomenon of variable range hopping with the temperature dependent DC conductivity

$$\sigma(T) \propto \exp[-(T_0/T)^{1/4}] \quad (5)$$

where T is the temperature of the system and T_0 is a constant that depends on the decay length of the exponentially localized states (α) and density of states at the Fermi level. Charge transport by thermally assisted hopping of electrons between localized states is the basic assumption in the derivation of the $T^{-1/4}$ law.

Starting from Mott’s model, Ambegaokar *et al* [21] derived the same temperature dependence of the conductivity [22]. The basic step in their evaluation of the conductivity is the reduction of the hopping model to an equivalent random resistance network as Miller

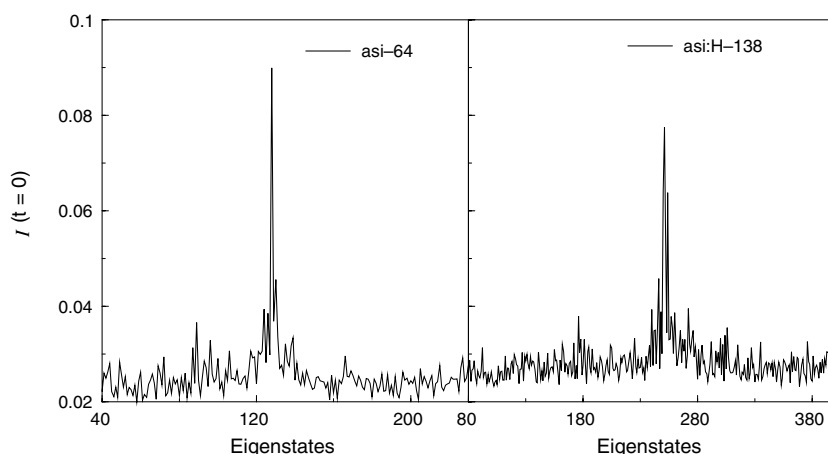


Figure 1. \mathcal{I} (localization) plotted against eigenvalue index for most of the states for asi-64 and asi:H-138 at time $t = 0$. The peak in \mathcal{I} shows strong localization. The Fermi level is near the eigenvector with maximum localization in both curves.

and Abrahams [4] reported earlier. In their model Miller and Abrahams showed that the hopping regime conductivity problem is equivalent to finding an effective resistance of a random impedance network in which each pair of centres i and j (the centres of localized electronic states) is connected by a resistance Z_{ij} whose inverse is given by

$$Z_{ij}^{-1} = \frac{e^2}{k_B T} n_i (1 - n_j) \Gamma_{ij}, \quad (6)$$

where Γ_{ij} is the transition rate for an electron hopping from centre i to j and may be approximated for a localized state with a single well defined centre and spherical symmetry as

$$\Gamma_{ij} = \begin{cases} v_0 \exp(-2\alpha_i R_{ij}) \exp[(E_i - E_j)/k_B T] & \text{if } E_i < E_j \\ v_0 \exp(-2\alpha_i R_{ij}) & \text{if } E_i > E_j \end{cases} \quad (7)$$

where v_0 is a constant which depends on phonon density of states, electron–phonon coupling strength and other properties of the material, R_{ij} is the distance between the centres i and j whose respective electronic energy levels are E_i and E_j (the resonance term), α_i^{-1} is the localization length that describes the spatial extent of the wavefunctions localized at centre i . n_i is the equilibrium occupation of centre i which is given by

$$n_i = (1 + \exp[(E_i - E_f)/k_B T])^{-1} \quad (8)$$

and E_f is the energy of the Fermi level.

3. Results

3.1. Spectral and spatial diffusion

The localization \mathcal{I} for the two models at $t = 0$ is depicted in figure 1. Highly localized states are clearly seen near the Fermi level. The values of \mathcal{I} for asi:H-138 are normalized with respect to the value of \mathcal{I} of asi-64.

To study the delocalization process in these models we chose two states near the Fermi level: the highest occupied molecular orbital (HOMO) and the lowest unoccupied molecular orbital (LUMO). For asi-64, the HOMO is a state which is localized around the dangling bond

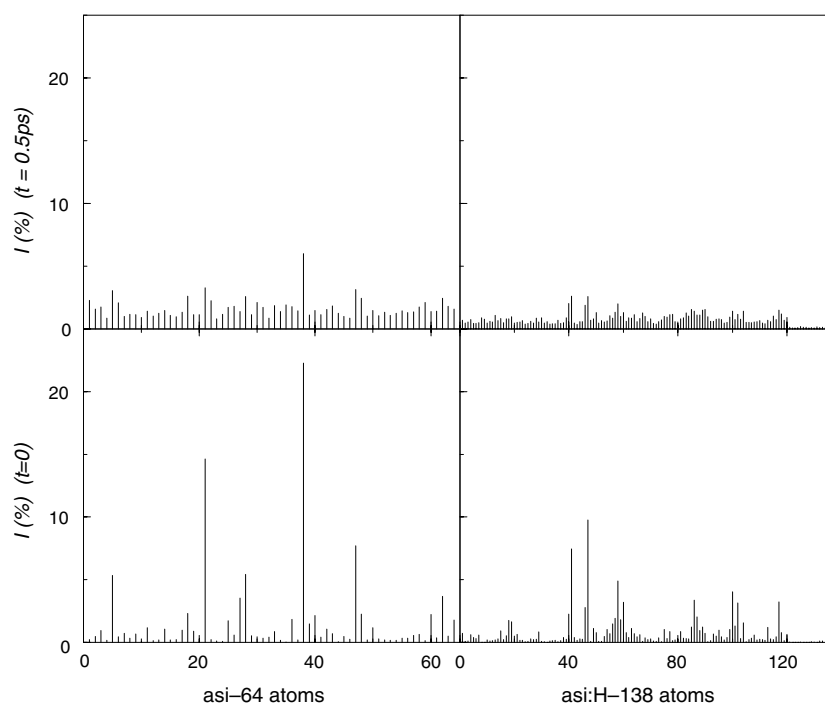


Figure 2. Spatial diffusion: contribution of each atom on the highest occupied molecular orbital (HOMO) in the case of asi-64, and lowest unoccupied molecular orbital (LUMO) in the case of asi:H-138, as a percentage at $t = 0$ and 0.5 ps, plotted against atom number.

with an energy splitting of 0.34 eV from the next occupied orbital and 0.88 eV below the LUMO. In the case of asi:H-138, the HOMO is an extended state with only 0.06 eV to the next occupied orbital and 1.53 eV below the bandtail localized state LUMO which is 0.11 eV below the next unoccupied state. These localized edge states are characterized by their higher \mathcal{I} value and concentration on a few atoms for both models at initial time $t = 0$, and diffuse as time goes on. To illustrate this, we calculated the contribution of every individual atom to \mathcal{I} of both states at $t = 0$ and 0.50 ps and in figure 2 we show the contribution of individual atoms for the localized states HOMO (for asi-64) and LUMO (for asi:H138). For asi-64, at $t = 0$ the HOMO state is localized mainly on the dangling bond atom with 23% contribution to the \mathcal{I} . This picture changes at a later time $t = 0.50$ ps, where the contribution of the dangling bond atom to \mathcal{I} drops to 6%. Similarly, for asi:H-138 the higher contribution to \mathcal{I} for the LUMO state changes from 10% at $t = 0$ to 2.60% at $t = 0.5$ ps.

Understanding how diffusion is driven by thermal disorder is the key to understanding the electronic dynamics and the hopping mechanism. Having this in mind we computed the time evolution of the two localized states, HOMO and LUMO, for three different temperatures 100, 300 and 500 K for both models we used and present the result in figure 3.

In both models we observed that increasing temperature increases the diffusion. In the case of asi-64 the HOMO takes about 0.2 ps and in case of asi:H-138 the LUMO takes about 0.15 ps to completely diffuse through the tiny cell at a temperature of 300 K. This diffusion is explained to be due to quantum mechanical mixing (resonant tunnelling) when other states get close in energy to the state that we are tracking. This is a manifestation of the ‘resonance condition’ [4] from direct calculation in our work.

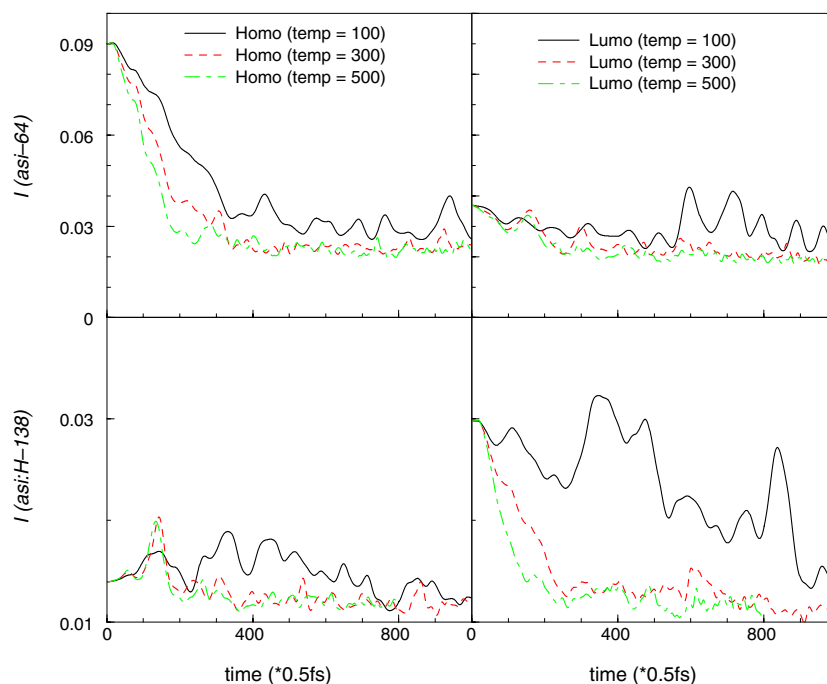


Figure 3. Thermally induced delocalization: the time evolution of the localization \mathcal{I} for highest occupied molecular orbital (HOMO) and lowest unoccupied molecular orbital (LUMO) of asi-64 and asi:H-138 respectively, at different temperatures.

The spectral diffusion of an electron state to a energy-adjacent state can be characterized by calculating the transition amplitude between the two states. The transition probability to the state η is $\rho(\eta) \propto |\langle C'_\eta(0) | C'(t) \rangle|^2$. Figure 4 shows the hopping probabilities from the initial LUMO state to the nearby states HOMO and LUMO + 1 in asi:H-138. It is evident from the energy difference of 1.53 eV between the HOMO and LUMO states in asi:H-138 that the hopping probability from one state to the other is very small and hence their spectral diffusion is very limited. On the other hand, the spectral diffusion from LUMO to LUMO + 1 (0.06 eV energy splitting) is larger. Elsewhere [23, 24], we have shown that the mixing proceeds via thermally driven resonant cluster proliferation [24]. In a subsequent calculation on a much larger system, the ‘island’ structure of localized states [24, 25] will be important. That is, the idealization of localized states having well defined single centres is *incorrect* for states sufficiently far into the band tails, but still on the localized side of the mobility edge. We note that the present calculation is not designed to properly model carrier trapping in localized states. To accomplish this, the trap must be unoccupied, and an electron in the conduction tail should be added and its time dependence studied.

Figure 4 may also be interpreted providing examples of the phonon-driven transitions (essentially equation (7)) for $\text{LUMO} \rightleftharpoons \text{HOMO}$ and $\text{LUMO} \rightleftharpoons \text{LUMO} + 1$, the latter transition being relevant to a weakly n-doped material. The interesting feature of these calculation is that there are no assumptions made as in Miller–Abrahams theory (such as simple radial exponential decay of wavefunctions, that the existence and character of the defect states arises from ‘real’ topological disorder and, perhaps most importantly, our localized states are not static, but rather are time dependent according to the detailed dynamics of the network). In subsequent work, we will report the use of these ‘*ab initio* transition probabilities’ for computing hopping

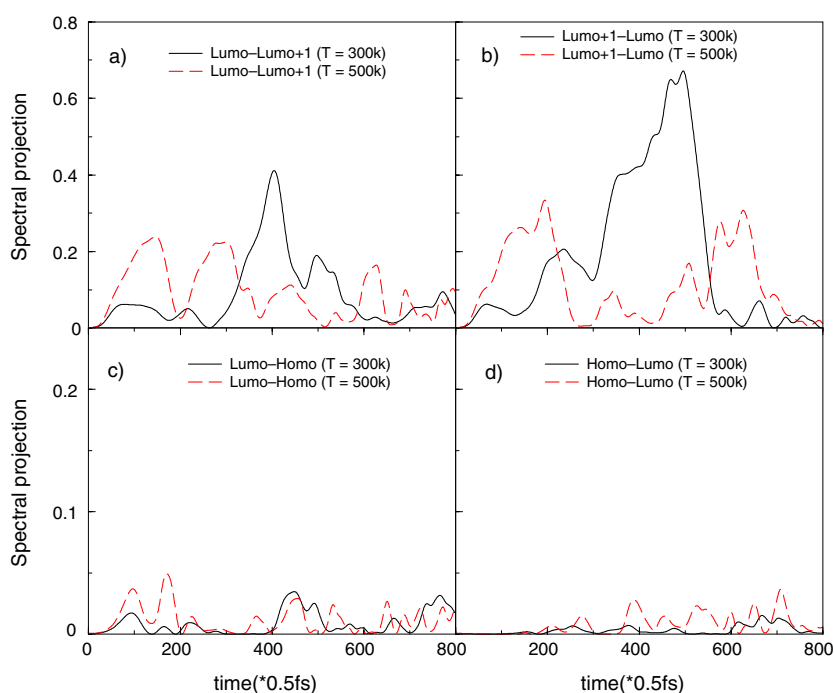


Figure 4. The spectral leakage of the selected states to the nearby states (and back) for asi:H-138 at different temperatures, giving examples of the hopping process between states.

conductivity. We have not yet fully implemented the Miller–Abrahams type picture, but we note that, in principle, all the ingredients are present in this work. It is also possible to imagine a very direct approach to transport in which we subject the supercell to an electric field (for simplicity in a slab geometry with the field transverse to the slab) and track the time development of electron packets.

4. Conclusion

We have presented a simulation of the dynamics of the localized states in the presence of thermal disorder by integrating the time-dependent Kohn–Sham equation. We have found that all localized states diffuse for sufficiently high temperatures and long timescales. The present work should be developed in various ways.

- (1) The case of a spin-polarized system should be considered. Such a calculation in the local spin density approximation should be directly comparable to electron paramagnetic resonance experiments, and should provide an interesting study in the differences between spin and charge diffusion [26].
- (2) Self-consistent field methods should be employed.
- (3) Larger model systems should be studied (to reduce admittedly serious finite-size effects).
- (4) The scheme should be applied to interesting molecular and biomolecular systems.

Acknowledgments

We thank Professor Pablo Ordejón for help with SIESTA, and many discussions. We also thank Professor Eric Schiff for helpful insights and advice. Finally, we thank the National Science

Foundation for support under grants DMR 0310933 and DMR 0205858 and P A Fedders for providing us with his unpublished a-Si:H model.

References

- [1] Thorpe M F and Weaire D 1971 *Phys. Rev. B* **4** 3518
Thorpe M F and Weaire D 1971 *Phys. Rev. Lett.* **27** 1581
Weaire D and Thorpe M F 1971 *Phys. Rev. B* **4** 2508
- [2] Ziman J M 1979 *Models of Disorder* (Cambridge: Cambridge University Press) p 457
- [3] Mott N F 1956 *Can. J. Phys.* **34** 1356
- [4] Miller A and Abrahams E 1960 *Phys. Rev.* **120** 745
- [5] Conwell E M 1956 *Phys. Rev.* **103** 51
- [6] Shklovskii B I and Efros A L 1984 *Electronic Properties of Doped Semiconductors* (Berlin: Springer)
- [7] Zallen R 1998 *The Physics of Amorphous Solids* (New York: Wiley-Interscience)
- [8] Atta-Fynn R, Biswas P and Drabold D A 2004 *Phys. Rev. B* **69** 245204
- [9] Lincoln A 1863 The hen is the wisest of all the animal creation because she never cackles until after the egg has been laid
- [10] Ordejón P, Artacho E and Soler J M 1996 *Phys. Rev. B* **53** 10441
- [11] Sánchez-Portal D, Ordejón P, Artacho E and Soler J M 1997 *Int. J. Quantum Chem.* **65** 453
- [12] Soler J M, Artacho E, Gale J D, García A, Junquera J, Ordejón P and Sánchez-Portal D 2002 *J. Phys.: Condens. Matter* **14** 2745
- [13] Perdew J P and Zunger A 1981 *Phys. Rev. B* **23** 5048
- [14] Troullier N and Martins J L 1991 *Phys. Rev. B* **43** 1993
- [15] Kleinman L and Bylander D M 1982 *Phys. Rev. Lett.* **48** 1425
- [16] Artacho E, Sánchez-Portal D, Ordejón P, García A and Soler J M 1999 *Phys. Status Solidi b* **215** 809
- [17] Tomfohr J K and Sankey O F 2001 *Phys. Status Solidi* **226** 115
- [18] Barkema G T and Mousseau N 2000 *Phys. Rev. B* **62** 4985
- [19] Fedders P A 2003 unpublished
- [20] Mott N F and Davis E A 1979 *Electronic Processes in Noncrystalline Materials* 2nd edn (Oxford: Clarendon)
- [21] Ambegaokar V, Halperin B I and Langer J S 1971 *Phys. Rev. B* **4** 2612
- [22] Mott N F 1984 *The Physics of Hydrogenated Amorphous Silicon II, Electronic and Vibrational Properties* vol 56 (Berlin: Springer) p 189
- [23] Li J and Drabold D A 2003 *Phys. Rev. B* **68** 033103 and references therein
- [24] Dong J J and Drabold D A 1998 *Phys. Rev. Lett.* **80** 1928
- [25] Ludlam J J, Elliott S R, Taraskin S N and Drabold D A 2004 unpublished
- [26] Atta-Fynn R, Biswas P, Ordejón P and Drabold D A 2004 *Phys. Rev. B* **69** 085287